

# In silico activation of Src tyrosine kinase reveals the molecular basis for intramolecular autophosphorylation<sup>☆</sup>

Jesús Mendieta<sup>1</sup>, Federico Gago\*

*Departamento de Farmacología, Universidad de Alcalá, E-28871 Alcalá de Henares, Madrid, Spain*

Received 3 January 2004; received in revised form 21 May 2004; accepted 3 June 2004

Available online 28 July 2004

## Abstract

Structural data suggest that important hinge-bending motions of the two lobes that shape the catalytic domain of Src tyrosine kinase, together with reorganization of an alpha helix (helix C), are needed for the activation loop to adopt the catalytically competent conformation. The phosphorylation of a Tyr residue (Tyr-416) in this loop also seems to be essential for enzyme activation. However, no information is available about the dynamics of this activation process. By comparing the inactive and active forms of the catalytic domains of Src and Lck, another member of the Src family, we first identified a short stretch that can act as a hinge for the interlobe motion. The opening of the lobes was then simulated using a targeted molecular dynamics approach. The results obtained suggested that pulling the two lobes apart is not enough to induce the required conformational change in the activation loop. Rather unexpectedly, however, swinging of the lobes situated Tyr-416 in a suitable position for intramolecular autophosphorylation, and further simulation of Tyr-416-phosphorylated Src in the presence of ADP did then result in a conformational change that placed the activation loop in a position similar to that found in the active open conformation of Lck. Taken together, our results establish a physical link between intramolecular autophosphorylation and loop activation. © 2004 Elsevier Inc. All rights reserved.

**Keywords:** Hinge motion; Targeted molecular dynamics; Tyrosine kinase; Autophosphorylation

## 1. Introduction

Cellular Src (c-Src) is the normal cellular counterpart of the product of the first oncogene identified from Rous sarcoma virus, v-Src, and also the first protein characterized as being able to phosphorylate tyrosine residues [1]. Src substrates are found in the cytosol or at the inner face of the plasma membrane, or at cell–matrix or cell–cell adhesions. Tyrosine phosphorylation of these proteins can affect their function directly or, alternatively, the phosphotyrosyl residues can serve as docking sites for the binding of signaling proteins containing SH2 domains. The resulting complexes then initiate pathways that regulate protein synthesis, gene expression, cytoskeletal assembly and many other aspects of cell function [2]. Because Src family members are involved in many signaling pathways by means of which sev-

eral surface receptors regulate cell growth and proliferation, their catalytic activity is strictly regulated [3], thus offering unique opportunities for modulation by small molecules in the fight against disease.

Src can also phosphorylate itself at tyrosine residues. Although the major *in vivo* phosphorylation site on platelet Src was shown to be Tyr-527, which acts as a negative regulator of its kinase activity [4] and is absent in v-Src, the major site of autophosphorylation *in vitro* is Tyr-416, a residue located at the center of the catalytic domain [5]. Phosphorylation of Tyr-416 in both v- and c-Src results in increased activation of the enzyme [6–8] whereas mutation of this residue to phenylalanine (Y416F) significantly reduces the transforming potential of Src [9]. A tyrosine kinase that specifically phosphorylates Src at Tyr-527, carboxy-terminal Src kinase (Csk), has been identified [10], as have phosphatases that can dephosphorylate this residue [11], highlighting the fact that the phosphorylation status of Tyr-527 is key for *in vivo* c-Src regulation. However, to the best of our knowledge, no tyrosine kinase specific for Src Tyr-416 has been described yet. Instead, an autophosphorylation mechanism has been proposed based on the finding that the level of phosphorylation of this tyrosine residue correlates with the activity of

<sup>☆</sup> Supplementary data associated with this article can be found, in the online version, at [doi:10.1016/j.jmgm.2004.06.001](https://doi.org/10.1016/j.jmgm.2004.06.001).

\* Corresponding author. Tel.: +34 918 854 514; fax: +34 918 854 591. E-mail address: [federico.gago@uah.es](mailto:federico.gago@uah.es) (F. Gago).

<sup>1</sup> Present affiliation: Centro de Biología Molecular “Severo Ochoa” C.S.I.C. Universidad Autónoma de Madrid, E-28049 Cantoblanco, Madrid, Spain.

the enzyme and its mutants [12]. Since autophosphorylation of purified, monomeric,  $\nu$ -Src was shown to be independent of its concentration, an intramolecular reaction was early proposed [13]. Nevertheless, intermolecular autophosphorylation is also possible because Src can be phosphorylated in cells expressing both the Y416F mutant enzyme and another mutant form that can be phosphorylated at Tyr-416 but cannot donate phosphate [14]. Since Tyr-416 lies within a region conserved in all members of the tyrosine kinase family named the activation loop, the phosphorylation of this residue could induce an important conformational change responsible for the activation of the enzyme.

The structural domains of Src kinase (and other members of the family) are, in order from the N-terminus: the SH4 (Src homology 4), SH3, SH2 and SH1 domains. SH1 is the catalytic domain, SH2 and SH3 are both molecular adhesives important for protein–protein interaction, and SH4 plays a role in membrane attachment. SH2 domains bind phosphotyrosine-containing peptides [15,16] whereas SH3 domains recognize proline-rich peptides [17]. Both SH2 and SH3 domains were early shown to be involved in the regulation of the kinase activity of Src [18,19]. The complex interactions between different domains of c-Src were better understood when the three-dimensional structures of c-Src [20], and the Src family tyrosine kinase Hck [21], were solved, both in a catalytically inactive conformation.

Each of these crystal structures revealed a finely adjusted nanomachine [2] in which all structural elements, i.e., the SH3 and SH2 domains, the linker between SH2 and SH1 domains, and the carboxy-terminal tail cooperate in order to keep the catalytic domain under control. As in all known kinases, the catalytic domain is made up of a small  $\alpha/\beta$  N-terminal lobe and a large  $\alpha$  C-terminal lobe. The linker joining the SH2 and the catalytic domain adopts a polyproline type II helix structure and serves as an adapter to fit together the N-terminal lobe and the SH3 domain. This conformation places the SH2 domain in a suitable position to bind the phosphotyrosine residue at the C-terminal tail (pTyr-527) which extends from the base of the catalytic domain. Binding of pTyr-527 to SH2 acts as a safety catch that locks the whole structure in an inactive conformation [2].

The overall structure of the catalytic domain, shaped as two lobes connected by a short polypeptidic strand, strongly suggests considerable interlobe mobility. In the inactive conformation the two lobes approach each other closely, and the interactions of SH1 with the SH2 and SH3 regulatory domains, the linker, and the C-terminal tail serve to bring the catalytic lobes close together thereby narrowing the cleft and preventing substrate-binding. In an ‘open’ active conformation [22], as that found in the crystal structure of the catalytic domain of Lck (another member of the Src family), the lobes are swung apart and the substrate-binding cleft is easily accessible, thus supporting the importance of structural mobility in Src regulation.

Lobe mobility could be essential for Src activation, not only to facilitate substrate recognition, but also to reorganize

the active site during catalysis. This kind of motion is common to many other enzymes and protein molecules [23], in which two or more domains are connected by a few strands of polypeptide chains that can be considered as hinges [24]. The conformational changes responsible for these motions are usually limited to the hinge region in so far as the domains behave as rigid bodies.

Dynamic hinge-bending motions in proteins are not easily amenable to experimental structural studies but molecular dynamics (MD) simulations provide a computational alternative that can help to gain insight into these processes at the atomic level. However, these motions take place at time scales that are more than one order of magnitude longer than those currently achieved by state-of-the-art MD simulations. This is so because the system must surmount the energy barrier that separates the open and the closed forms. Thus, even though the energy-barrier crossing process itself is normally quite fast, the time required for random thermal fluctuations within the system to produce the local atomic momenta required for overcoming the local energy barrier may be of the order of milliseconds or longer. In these cases, a targeted MD (tMD) approach [25] can be used to accelerate the process and simulate the subdomain hinge-bending motion. This approach has been previously used to study conformational changes in several proteins such as the GroEl chaperone [26] and the glutamate receptor ligand-binding core [27], as well as the coupling between SH2 and SH3 domains when Src is forced to adopt the open conformation [28].

In the following, we focus our attention on the dynamic properties of the catalytic domain itself. We first study its molecular architecture to pinpoint the mobile parts responsible for the interlobe motion. We then simulate the hinge-bending motion using tMD to explore how the conformational change in the activation loop is triggered, and in doing so we also probe the feasibility of an intramolecular mechanism for Tyr-416 autophosphorylation.

## 2. Results and discussion

### 2.1. Determination of the hinge regions of Src catalytic domain

Evidence for a hinge-bending motion associated with the activation of the Src catalytic domain can be gained from comparison of the crystal forms of non-active Src [20] and active Lck catalytic domains [22]. Visual inspection of these structures shows that, irrespective of changes in interlobe orientation and activation loop conformation, the overall structure of each lobe is maintained upon activation (Fig. 1).

Alignment of the catalytic domains of Src and Lck also shows that not only do they share significant sequence homology (>64%) but also very high structural homology. In fact, only 10 out of 263 C $\alpha$  atoms of the catalytic domain are in non-equivalent positions, and all of these residues without structural homology precisely belong to the activation

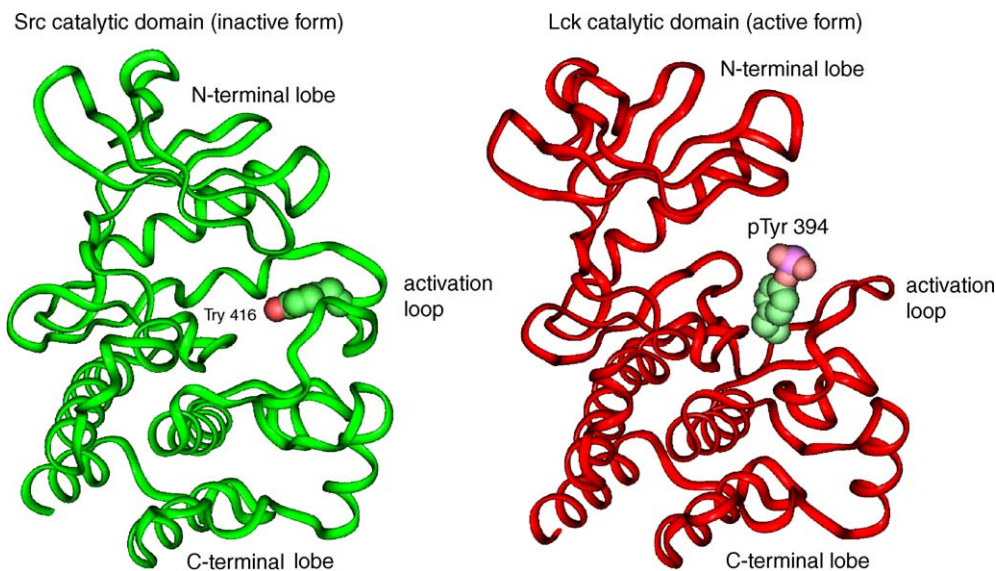


Fig. 1. Comparison of the overall structures of the catalytic domains of the human tyrosine kinase Src in a closed inactive conformation (green ribbon, PDB code 2SRC), and human lymphocyte kinase, Lck, in an open active conformation (red ribbon, PDB code 3LCK).

loop. The root-mean-square deviation (rmsd) between the  $C\alpha$  traces of the Src and Lck catalytic domains, excluding the activation loop, is 2.49 Å, which is higher than that obtained when the structures of Src and Hck catalytic domains (both in an inactive form) are compared (rmsd = 1.0 Å). However, when considered separately, the rmsd between the  $C\alpha$  traces of the N- and C-terminal lobes (excluding the activation loop) of Src and Lck are 1.12 and 0.98 Å, respectively. These results confirm that, despite the overall conformational change, the two lobes do indeed behave mostly as rigid bodies.

More precise information about the mobile parts of the Src catalytic domain can be obtained either by comparing pairs of phi–psi angles for each residue or, more simply, by calculating the differences between equivalent dihedral angles of the  $C\alpha$  traces of ‘active’ Lck and ‘inactive’ Src (Fig. 2):

- (i) The first region in which a difference between the dihedral angles of  $C\alpha$  traces of the closed (Src) and open (Lck) forms is observed corresponds to a segment of the Gly-rich loop (residues 273–278; a in Fig. 2) that makes up part of the ATP-binding site (see also Fig. 10).
- (ii) The next variation ( $b_1$  and  $b_2$ , in Fig. 2) is detected just before and after the residues corresponding to the only helix present in the N-terminal lobe (residues 304–316), but the helical structure itself (helix C) is completely conserved. This means that helix C can be reoriented without changing its secondary structure. More interesting are the differences in the conformation corresponding to the region that connects the two lobes of the catalytic domain (residues 341–359; c in Fig. 2). This region is adjacent to the loop that is involved in the recognition of the adenine moiety of ATP, and

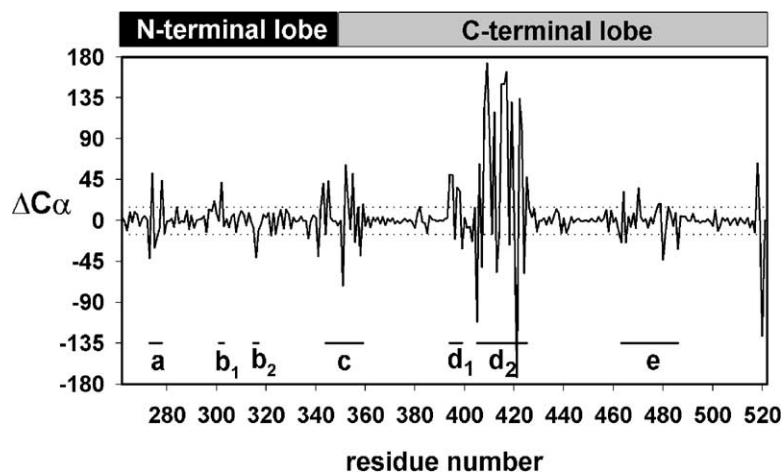


Fig. 2. Differences in  $C\alpha$  dihedral angles ( $\Delta C\alpha$ ) along the peptide backbone between the open and closed forms shown in Fig. 1. Residue numbering refers to human Src. The horizontal dashed lines represent the mean of the difference for all residues  $\pm 2\sigma$ .

comprises a short helix flanked by two short strands. This structural element appears suitable for performing the role of a hinge as small changes in the helical angles can give rise to relatively large displacements of the strands (Fig. 11). This peculiar structure, together with the fact that it is located at the interlobe boundary, strongly suggest that the conformational changes in this region could be responsible for the differences found in the relative orientation of the two lobes between the non-active Src structure and the open active conformation of Lck.

- (iii) The most remarkable differences, however, are found, as expected, between residues 394 and 425 (regions  $d_1$  and  $d_2$ , Fig. 2). A short segment of this region corresponds to a loop that is in contact with the SH2 domain ( $d_1$ , residues 294–299), but the segment where the difference is the highest corresponds to the activation loop ( $d_2$ , residues 405–425).
- (iv) The last region for which significant differences are found between the  $C\alpha$  trace dihedral angles of closed and open forms (residues 483–496, e in Fig. 2) has no associated function in Src although a homologous region in glycogen synthase kinase, Gsk3, corresponds to the FRATtide peptide-binding site [29].

## 2.2. Stability of the Src holoenzyme

Since both Src and Lck crystal structures have been obtained in the absence of bound ATP or one of its non-hydrolyzable analogues, we placed an ATP molecule in the nucleotide binding site of Src in such a way that it resembled the conformation and orientation found in the crystal structure of cAMP-dependent protein kinase [30]. We also placed two  $Mg^{2+}$  ions in the positions occupied by the two  $Mn^{2+}$  ions in this structure even though it is known that only one is essential for kinase activity [31]. The holoenzyme was then solvated as described in the Section 3, and the behaviour of the whole system was simulated.

No significant conformational changes in the protein were detected during the 2-ns trajectory. The rmsd value of  $C\alpha$  atoms with respect to the initial structure was never higher than 1.25 Å (Fig. 3). At the beginning of the simulation, three water molecules were incorporated to the coordination spheres of the metal ions. As seen for  $Mn^{2+}$  in cAMP-dependent protein kinase, one of the  $Mg^{2+}$  ions is coordinated in a rather regular octahedral coordination sphere by the two oxygens of the  $\beta$  and  $\gamma$  phosphoryl groups of ATP, the two carboxylate oxygens of Asp-404, and two water molecules. The other  $Mg^{2+}$  ion is coordinated in an unusual trigonal bipyramidal geometry by two oxygens from the  $\alpha$  and  $\gamma$  phosphoryl groups of ATP, one carboxylate oxygen from Asp-404, the oxygen from the side chain of Asn-391, and a water molecule. These coordination spheres were consistently observed during the whole trajectory, and both distances and angles were similar to those found for  $Mn^{2+}$  in the cAMP-dependent protein kinase crystal structure (data not shown).

The relative position of ATP in the protein did not change with respect to the initial orientation and differs from that found for  $Ca^{2+}$ -bound 5' adenylyl-imido-triphosphate in the crystal structure of the Src family tyrosine kinase Hck [21] only in the position of the  $\gamma$  phosphate group, as expected from the differences observed in metal ion–phosphate coordination.

## 2.3. Simulation of Src catalytic domain activation

In order to preserve the characteristics of a typical hinge-bending motion, the overall shapes of the N- and C-terminal lobes were maintained during the tMD simulation by restraining the dihedrals of their  $C\alpha$  traces in the non-mobile regions to the values found in the inactive form of the enzyme, as explained in the Section 3. The hinge motion was 'activated' by forcing the  $C\alpha$  trace of the residues making up the hinge region of Src to adopt the conformation found for the equivalent stretch in the open conformation of Lck. Fig. 4a shows the evolution of the rmsd value of  $C\alpha$

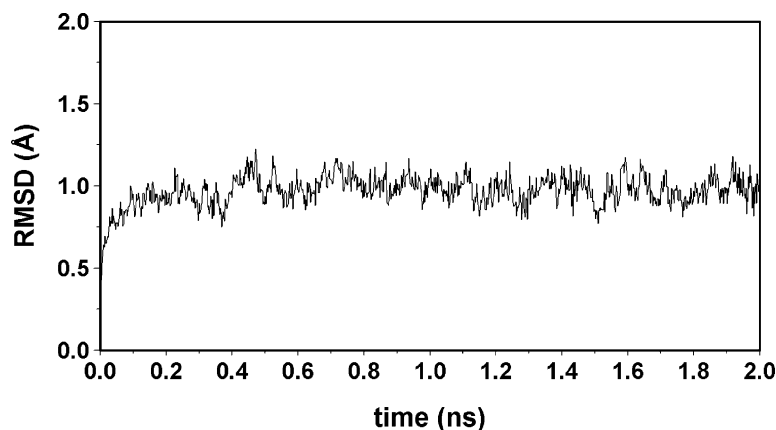


Fig. 3. Root-mean-square deviation (RMSD) of  $C\alpha$  atoms belonging to the Src catalytic domain in its complex with ATP/ $2Mg^{2+}$  along the simulation time with respect to the initial modelled structure.

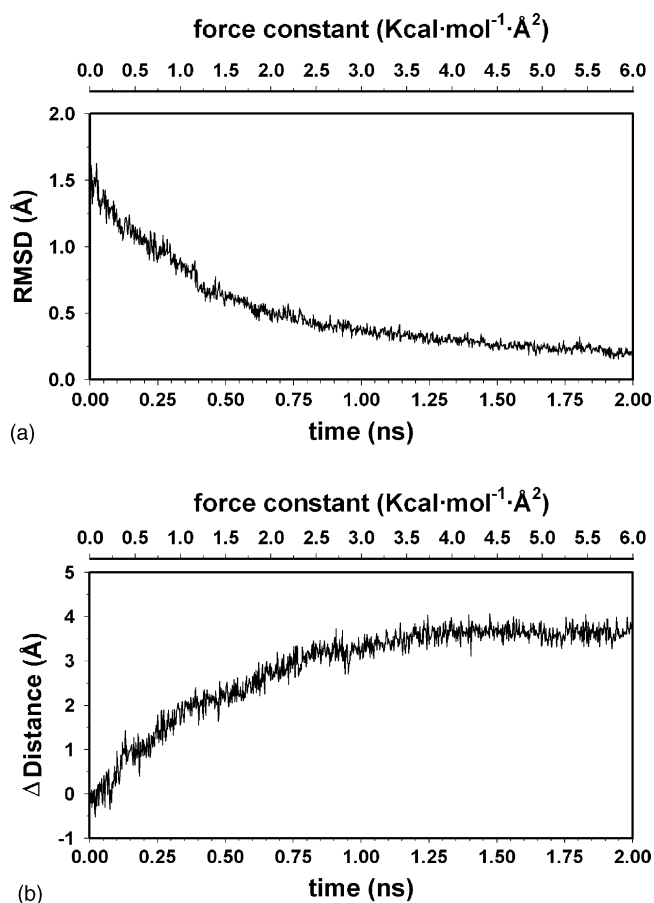


Fig. 4. Monitoring of the hinge-bending motion during interlobe separation along the simulation time. (a) RMSD of C $\alpha$  atoms belonging to the hinge region (residues 341–359) of Src with respect to equivalent residues in the Lck open active conformation. (b) Interlobe separation measured as the distance between C $\alpha$  atoms corresponding to residues Pro-333 and Thr-440, each placed in a different lobe. The upper axis in both panels shows the value of the template force constant applied at different times during the simulation.

atoms of the hinge (residues 341–359) with respect to the corresponding atoms in the open ‘active’ conformation of Lck along the simulation time. The adaptive conformational changes in the hinge region are apparent even at very low force constant values and the rmsd becomes progressively and gradually reduced as the force constant applied to the system increases until it reaches a value very close to zero at the end of the simulation.

The hinge-based separation of the N- and C-terminal lobes of the Src catalytic domain was also monitored by measuring the distance between C $\alpha$  atoms corresponding to residues Pro-333 and Thr-440, each placed in a different lobe (Fig. 4b). This increase in interlobe distance nicely correlates with the extent of the overall conformational change in the hinge region (Fig. 4a). For values above 3.55 kcal mol<sup>-1</sup> per hinge atom the distance reaches a plateau, which corresponds to the degree of opening found in ‘active’ Lck. Taken together, these results strongly suggest that interlobe separation in the Src catalytic domain is induced by a confor-

mational change taking place solely in a short polypeptide stretch close to the region that connects the two lobes.

The aim of this work was to understand whether the hinge-bending motions of the lobes are associated with the conformational changes in the activation loop that result in Src catalytic domain activation. In the closed inactive form, the activation loop is packed close to the substrate-binding cleft (Fig. 1) and not far from the active site of the enzyme. Some residues of this loop establish interactions with helix C. For example, Arg-409 forms a salt bridge with Glu-310 whereas in the open active structure the carboxylate of this glutamate residue forms a salt bridge with the  $\epsilon$ -amino group of Lys-295, a residue that is involved in the recognition of the phosphate groups of ATP. Current hypotheses based on structural data [20,21] suggest that the interlobe opening motion could give rise to the reorientation of helix C allowing the conformational changes in the activation loop to take place.

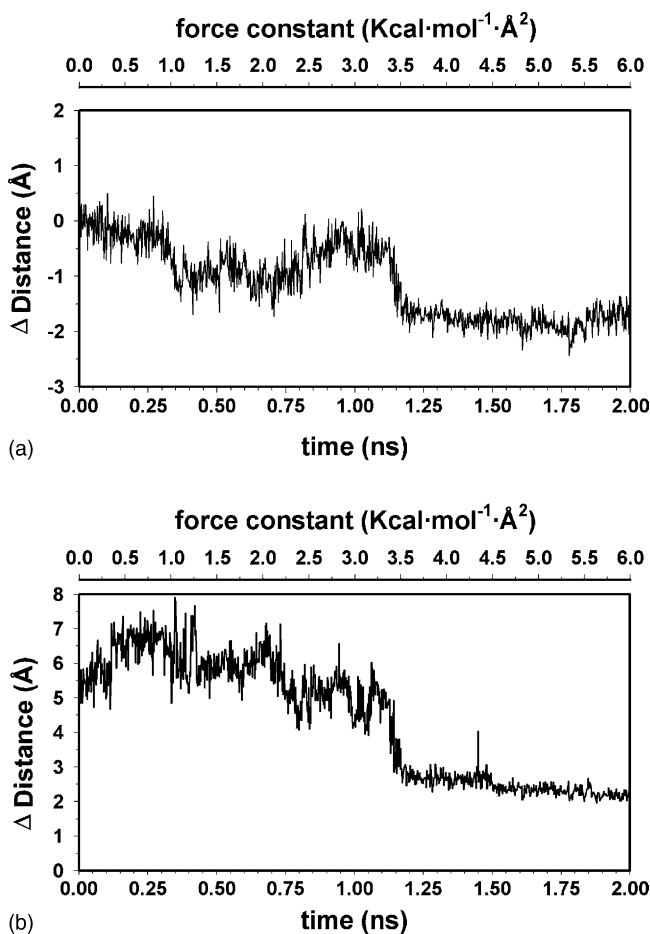


Fig. 5. Monitoring of the conformational changes affecting the activation loop. (a) Distance between the C $\alpha$  atoms of Asn-391, placed at the cleft, and the phosphorylatable Tyr-416 located on the activation loop. (b) Distance between the phenolic oxygen of Tyr-416 and the Mg<sup>2+</sup> ion that is coordinated by the  $\beta$  and  $\gamma$  phosphoryl oxygens of ATP. The upper axis in both panels shows the value of the template force constant applied at different times during the simulation.

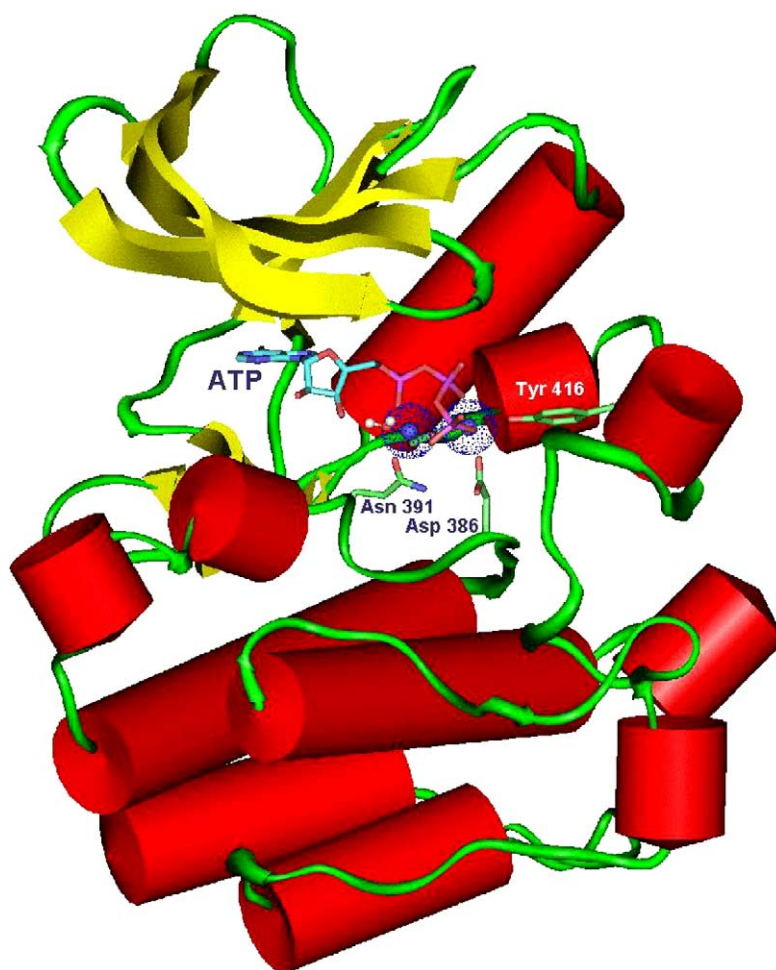


Fig. 6. Schematic representation of the energy-minimized average structure of Src catalytic domain from the last 500 ps of the targeted molecular dynamics simulation. All water molecules but one have been removed for clarity.

This rearrangement was monitored by the increase in the distance between the C $\alpha$  atoms of Asn-391, a residue that is involved in the binding of the ATP/2Mg<sup>2+</sup> complex, and the phosphorylatable Tyr-416 at the activation loop itself (Fig. 5a). However, under our simulation conditions, the activation loop did not swing away from the cleft. On the contrary, this interresidue distance decreased, suggesting that lobe separation favours the packing of the activation loop within the cleft. The interaction between residues of the activation loop and helix C, most notably the salt bridge between Arg-409 and Glu-310, was not disrupted during the simulation either. As a consequence, the motion of the N-terminal lobe dragged the side chains of the activation loop residues deeper into the cleft. To illustrate this, Fig. 5b shows the distance between the phenolic oxygen of Tyr-416 and the Mg<sup>2+</sup> ion that is coordinated by the  $\beta$  and  $\gamma$  phosphoryl oxygens of ATP. At the end of the tMD simulation, by the time the two lobes are as separated as in the ‘active’ conformation (Fig. 6), the phenolic oxygen of Tyr-416 is only 2 Å away from the Mg<sup>2+</sup> indicating that it has been incorporated into its coordination sphere by displacing a water molecule. Similarly, a second water molecule that also was coordi-

inating the Mg<sup>2+</sup> ion has been simultaneously replaced by one of the carboxyl oxygen of Asp-386 (Fig. 7). Coincidentally, the Mg<sup>2+</sup> that is coordinated by the phosphorylatable oxygen of Tyr-416 has been postulated to be the essential ion for catalysis [32], and Asp-386 is a residue that is conserved in all protein kinases and is most likely involved in the catalytic mechanism [33]. The final structure obtained for the activated Src holoenzyme is thus strongly suggestive of an intramolecular mechanism for autophosphorylation at Tyr-416.

#### 2.4. Molecular dynamics simulation of the Tyr-416-phosphorylated kinase domain and ADP

Since the hydroxyl group of Tyr-416 was placed in a position suitable for intramolecular phosphorylation, we used the final structure of the previous complex to model the catalytic domain with a phosphotyrosine at position 416 and ADP in place of ATP, i.e., the immediate products of the reaction. The dynamic behaviour of this new complex was then simulated for 2 ns under the same conditions as before.

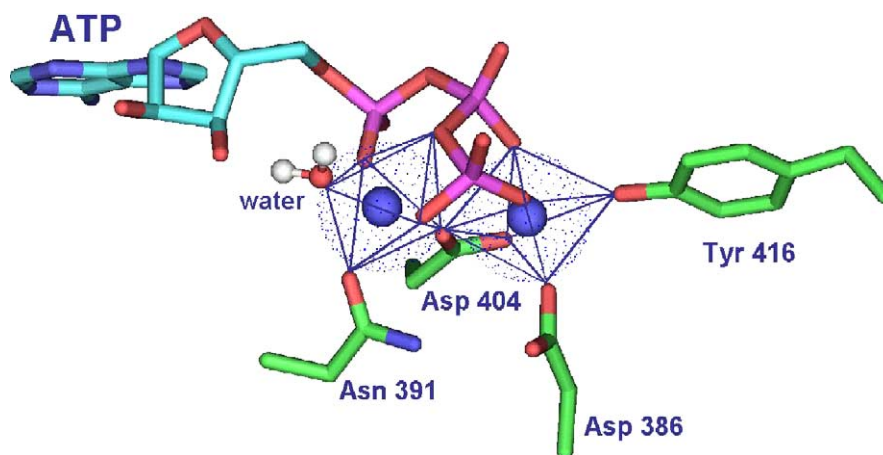


Fig. 7. Detailed view of the positions of the two bound  $Mg^{2+}$  ions (small blue spheres enveloped in a dotted surface) as found in the energy-minimized average structure of Src catalytic domain from the last 500 ps of tMD simulation. Only the ATP (sticks, carbon atoms colored cyan), the water molecule (ball and stick), and the side chains of those amino acids involved in metal complexation (sticks, carbon atoms colored green) are shown. The two octahedra have been drawn to highlight the bipyramidal coordination of the two ions.

The motion of the activation loop was studied by monitoring the separation between the  $C\alpha$  atoms of Asn-391 and pTyr-416 (Fig. 8). A sharp increase of this distance can be seen after about 50 ps, and a steady increase is observed until a plateau is reached at around 0.8 ns. This change comes mostly as a consequence of both the repulsion between the phosphate groups of ADP and the phosphotyrosine and the tendency of these groups to be surrounded by a solvation shell. The final distance is now very similar to that observed in the active open conformation of Lck. In fact, at the end of the simulation, the activation loop does indeed adopt the more extended conformation (Fig. 9) that is observed in the crystal structure of Lck (Fig. 1). Furthermore, in good analogy to what is seen in this experimental structure, the phosphate group of pTyr-416 is involved in two salt bridges with the guanidinium groups of Arg-385 and Arg-404, and another salt bridge is formed between the side chains of Glu-310 and Lys-295 (Fig. 9). It is precisely the interaction

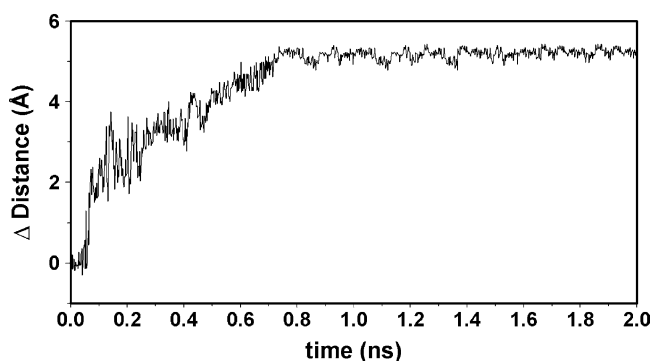


Fig. 8. Distance between the  $C\alpha$  atoms of Asn-391 and pTyr-416 along the simulation of the phosphotransfer reaction products. Note the difference with respect to the same distance measured in the pre-reaction complex as shown in Fig. 5a.

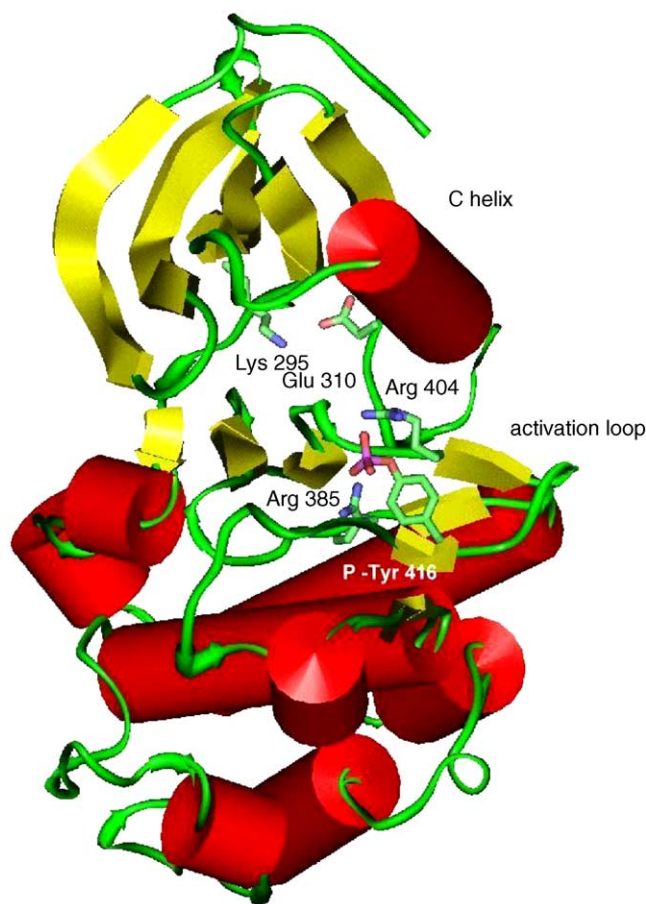


Fig. 9. Schematic representation of the energy-minimized average structure of the ADP-bound pTyr-416-Src catalytic domain from the last 1 ns of the simulation. Water molecules have been removed for clarity.

between residues equivalent to Glu-310 and Lys-295 that has been related to the activation, not only of tyrosine kinases [20,21], but also of Ser/Thr kinases [30].

### 3. Computational methods

#### 3.1. Atomic data

The atomic coordinates of human tyrosine kinase, c-Src [20], and human lymphocyte kinase, Lck [22], were obtained from the protein data bank (PDB codes: 2SRC and 3LCK, respectively). Both proteins were structurally aligned with the DALI software [35]. Differences in dihedral angles between the  $\alpha$ -carbon ( $C\alpha$ ) traces of open and closed forms were measured, with positive and negative values representing, respectively, clockwise and anticlockwise increments relative to the closed form.

Neither ATP nor ADP nucleotides were present in any of these PDB files. The ATP molecule and two  $Mg^{2+}$  ions were placed in the X-ray Src structure by superimposing those residues involved in ATP binding with equivalent residues from the crystal structure of cAMP-dependent protein kinase (PDB code: 1CDK) which has been co-crystallized with the non-hydrolyzable ATP analogue adenylyl imidodiphosphate [30]. Electrostatic potential-derived charges for ATP and ADP (Supplementary Material) were obtained

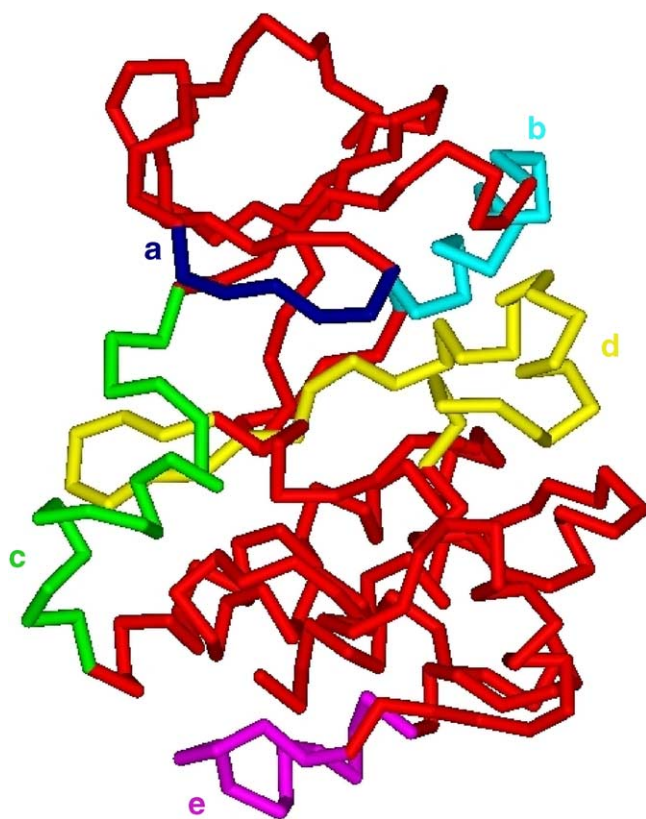


Fig. 10.  $C\alpha$  trace of Src tyrosine kinase catalytic domain highlighting in different colors the structural regions (a)–(e) depicted in Fig. 2.

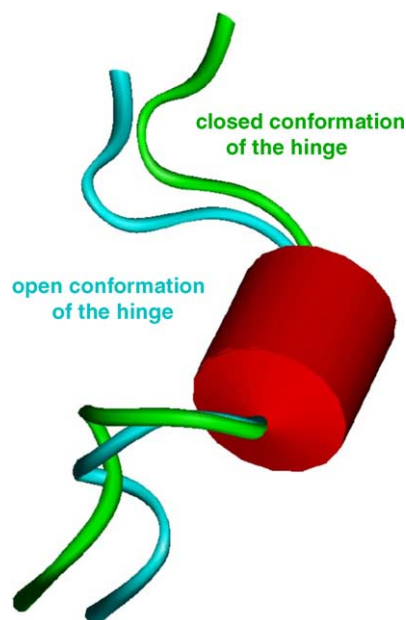


Fig. 11. Detailed view of the hinge region in both the open (cyan ribbon) and closed (green ribbon) forms of the Src holoenzyme. Helix C (red cylinder) has been used for superimposing both structures so as to highlight stand displacements.

with the RESP methodology [36] using a 6-31G\* basis set as implemented in the Gaussian-98 program [37]. Standard Lennard–Jones AMBER parameters [38] and a charge of +2 were used for  $Mg^{2+}$  ions. We used reported bonded and non-bonded parameters for the phosphotyrosine residue [28]. A spherical cap of TIP3P water molecules [39] centered on the  $C\alpha$  of Asp-404, located at the interlobe cleft, was used to simulate the aqueous environment. The 28 Å radius of this water cap was long enough to cover all residues of the activation loop in both active and inactive conformations.

#### 3.2. Energy refinement

To adapt the crystal structure to the AMBER force field [38], and to gradually refine the modelled Src-ATP-2 $Mg^{2+}$  complex, the SANDER module in AMBER [40] was employed for energy minimization using a cutoff of 10.0 Å. First, only the water dipoles were allowed to reorientate in the electric field of the holoenzyme; then the ATP and  $Mg^{2+}$  ions were also allowed to relax; subsequently, the amino acid side chains were also included in the energy refinement, and finally the whole structure was energy-minimized although protein backbone atoms were restrained to their initial positions with a force constant of 2 kcal mol<sup>-1</sup> Å<sup>-2</sup>. Each refinement stage consisted of 2000 steps of steepest descent and 8000 steps of conjugate gradient energy minimization.

#### 3.3. Molecular dynamics simulations

The refined holoenzyme was used as input for the subsequent MD simulations using the same cutoff as above. In

a 6 ps heating phase the temperature was raised from 0 to 298 K, and velocities were reassigned at each new temperature according to a Maxwell–Boltzmann distribution. ATP and  $Mg^{2+}$  ions were completely free to move. The  $C\alpha$  atoms of the C-terminal lobe were restrained to their initial positions with a force constant of  $2 \text{ kcal mol}^{-1} \text{ \AA}^{-2}$  (*positional restraints*) except for residues in the activation loop. The dihedral angles of the  $C\alpha$  trace of the N-terminal lobe region considered as a rigid body (see below) were restrained to those found in the initial structure (although a fluctuation of  $\pm 20^\circ$  was allowed) by means of a harmonic potential with a force constant of  $300 \text{ kcal mol}^{-1} \text{ rad}^{-2}$  (*dihedral restraints*). Identical restraints were applied to the hinge region for the first 500 ps of the simulation but they were removed thereafter, and the MD simulation was continued during 2 ns at the same temperature. The SHAKE algorithm was applied to constrain all bonds to their equilibrium values so that an integration time step of 2 fs could be used throughout. The list of non-bonded pairs was updated every 25 steps, and coordinates were saved every 2 ps.

The tMD approach consisted of forcing the  $C\alpha$  atoms of the hinge region of the ‘closed’ structure to adopt the crystallographic positions of equivalent atoms in the ‘open’ structure by means of a harmonic potential with a force constant that was progressively increased ( $0.25 \text{ kcal mol}^{-1} \text{ \AA}^{-2}$  per run) during 10 consecutive runs of 60 ps each. The incremental use of this term, as previously reported for another system [27], tends to avoid biasing the trajectory by overcoming artifactual energy barriers that could deprive the simulation of any physical sense.

For the simulation of pTyr-416-Src in the presence of ADP, the dihedral angles defining the  $C\alpha$  trace of hinge-region residues were restrained with a force constant of  $3.55 \text{ kcal mol}^{-1} \text{ \AA}^{-2}$  per atom in order to keep the interlobe cleft open.

#### 4. Conclusions

The overall molecular architecture of the catalytic domain of all protein kinases, which is shaped as two lobes connected by a short polypeptidic strand, reveals a remarkable plasticity [34] and strongly suggests considerable interlobe mobility. Comparison of Src in a closed inactive form and Lck in an open active conformation provides structural evidence that the motion of the lobes is an important event in the activation of the catalytic domain. The lobes behave essentially as rigid bodies, with most of the conformational changes being restricted to the activation loop and a short interlobe region that is best described as a hinge. Thus, activation of the catalytic domain of Src kinase has all the characteristics of a typical hinge-bending motion similar to that described for a number of other proteins [24].

Following the precise identification of this hinge region in Src, a tMD approach was used to pull the two lobes of the catalytic domain apart. Monitoring both the rmsd of the

hinge region relative to the open active conformation and the interlobe distance along the simulation showed that the conformational change taking place in this small stretch was enough for the two lobes to swing apart. However, the activation loop did not reach a conformation similar to that found in the active form. On the contrary, this segment was packed even deeper within the cleft. In this location, the phenolic oxygen of the phosphorylatable Tyr-416 was dragged into the coordination sphere of one of the ATP-bound  $Mg^{2+}$  ions. This placed the hydroxyl group at short distances of both the carboxylate of the catalytic Asp-386 and the  $\gamma$ -phosphate group of ATP, in a position suitable for attack. When the simulation proceeded with the immediate products of the phosphotransfer reaction, i.e., a phosphotyrosine at position 416 and ADP in the nucleotide binding site, the Src catalytic domain finally achieved a conformation similar to that observed in the crystal structure of Lck.

Taken together, our results support the feasibility of an intramolecular mechanism for the autophosphorylation of Tyr-416 [5,13], and further suggest that the conformational change in the activation loop responsible for kinase activation is triggered by this event rather than by the mere opening of the lobes.

#### Acknowledgements

J.M. is the recipient of a research fellowship from Comunidad de Madrid. We thank the University of Alcalá Computing Centre and the CIEMAT (Madrid) for generous allowances of computer time on their SGI servers. Financial support from the Spanish CICYT (SAF2003-07219-C02) and the National Foundation for Cancer Research is gratefully acknowledged.

#### References

- [1] T. Hunter, B.M. Sefton, Transforming gene product of Rous sarcoma virus phosphorylates tyrosine, Proc. Natl. Acad. Sci. USA 77 (1980) 1311–1315.
- [2] G.S. Martin, The hunting of Src, Nat. Rev. Mol. Cell Biol. 3 (2001) 467–475.
- [3] S.R. Hubbard, J.H. Till, Protein tyrosine kinase structure and function, Annu. Rev. Biochem. 69 (2000) 373–398.
- [4] J.A. Cooper, K.L. Gould, C.A. Cartwright, T. Hunter, Tyr527 is phosphorylated in pp60c-src: implications for regulation, Science 231 (1986) 1431–1434.
- [5] D. Feder, J.M. Bishop, Purification and enzymatic characterization of pp60c-src from human platelets, J. Biol. Chem. 265 (1990) 8205–8211.
- [6] J.E. Smart, H. Oppermann, A.P. Czernilofsky, A.F. Purchio, R.L. Erikson, J.M. Bishop, Characterization of sites for tyrosine phosphorylation in the transforming protein of Rous sarcoma virus (pp60v-src) and its normal cellular homologue (pp60c-src), Proc. Natl. Acad. Sci. USA 78 (1981) 6013–6017.
- [7] T. Patschinsky, T. Hunter, F.S. Esch, J.A. Cooper, B.M. Sefton, Analysis of the sequence of amino acids surrounding sites of tyrosine phosphorylation, Proc. Natl. Acad. Sci. USA 79 (1982) 973–977.

- [8] G. Sun, L. Ramdas, W. Wang, J. Vinci, J. McMurray, R.J.A. Budde, Effect of autophosphorylation on catalytic and regulatory properties of tyrosine kinase Src, *Arch. Biochem. Biophys.* 397 (2002) 11–17.
- [9] R. Ferracine, J. Brugge, Analysis of mutant forms of the c-src gene product containing a phenylalanine substitution for tyrosine 416, *Oncogene Res.* 5 (1990) 205–219.
- [10] M. Okada, H. Nakagawa, A protein tyrosine kinase involved in regulation of pp60c-src function, *J. Biol. Chem.* 264 (1989) 20886–20893.
- [11] S.A. Courtneidge, Activation of the pp60c-src kinase by middle T antigen binding or by dephosphorylation, *EMBO J.* 4 (1985) 1471–1477.
- [12] H. Piwnicka-Worms, K.B. Saunders, T.M. Roberts, A.E. Smith, S.H. Cheng, Tyrosine phosphorylation regulates the biochemical and biological properties of pp60c-src, *Cell* 49 (1987) 75–82.
- [13] Y. Sugimoto, E. Erikson, Y. Graziani, R.L. Erikson, Inter- and intramolecular interactions of highly purified Rous sarcoma protein pp60c-src, *J. Biol. Chem.* 260 (1985) 13838–13843.
- [14] J.A. Cooper, A. MacAuley, Potential positive and negative autoregulation of p60c-src by intermolecular autophosphorylation, *Proc. Natl. Acad. Sci. USA* 85 (1988) 4232–4236.
- [15] M. Masuda, B.J. Mayer, Y. Fukui, H. Hanafusa, Binding of transforming protein p47gag-crk to a broad range of phosphotyrosine-containing proteins, *Science* 248 (1990) 1537–1539.
- [16] M.F. Moran, C.A. Koch, D. Anderson, C. Ellis, L. England, G.S. Martin, T. Pawson, Src homology region 2 domains direct protein–protein interaction in signal transduction, *Proc. Natl. Acad. Sci. USA* 87 (1990) 8622–8626.
- [17] R. Ren, B.J. Mayer, P. Cicchetti, D. Baltimore, Identification of a ten-amino acid prolin-rich SH3 binding site, *Science* 259 (1993) 1157–1161.
- [18] S.M. Murphy, M. Bergman, D.O. Morgan, Suppression of c-Src activity by C-terminal Src kinase involves the c-Src SH2 and SH3 domains: analysis with *Saccharomyces cerevisiae*, *Mol. Cell Biol.* 13 (1993) 5290–5300.
- [19] G. Superti-Furga, S. Fumagalli, M. Koegl, S.A. Courtneidge, G. Draetta, Csk inhibition of c-Src activity requires both the SH2 and SH3 domains of Src, *EMBO J.* 12 (1993) 2625–2634.
- [20] W. Xu, S.C. Harrison, M.J. Eck, Three-dimensional structure of the tyrosine kinase c-Src, *Nature* 385 (1997) 595–602.
- [21] F. Sicheri, I. Moarefi, J. Kuriyan, Crystal structure of the Src family tyrosine kinase Hck, *Nature* 385 (1997) 602–609.
- [22] H. Yamagushi, W.A. Hendrickson, Structural basis for activation of the human lymphocyte kinase Lck upon tyrosine phosphorylation, *Nature* 384 (1996) 484–489.
- [23] M. Gerstein, W. Krebs, A data base of macromolecular motions, *Nucl. Acid Res.* 15 (1998) 4280–4290.
- [24] M. Gerstien, A.M. Lesk, C. Chothia, Structural mechanisms for domain movements in proteins, *Biochemistry* 33 (1994) 6739–6749.
- [25] J.A. McCammon, M. Karplus, Dynamics of activated processes in globular proteins, *Proc. Natl. Acad. Sci. USA* 76 (1997) 3585–3592.
- [26] J.P. Ma, P.B. Sigler, Z.H. Xu, M.A. Karplus, A dynamic model for the allosteric mechanism of GroEL, *J. Mol. Biol.* 302 (2000) 303–313.
- [27] J. Mendieta, G. Ramirez, F. Gago, Molecular dynamics simulation of the conformational changes of the glutamate receptor ligand-binding core in the presence of glutamate and kainate, *Proteins* 44 (2001) 460–469.
- [28] M.A. Young, S. Gonfloni, G. Superti-Furga, B. Roux, J. Kuriyan, Dynamic coupling between the SH2 and SH3 domains of c-Src and Hck underlies their inactivation by C-terminal tyrosine kinase phosphorylation, *Cell* 105 (2001) 115–126.
- [29] B. Bax, P.S. Carter, C. Lewis, A.R. Guy, A. Bridges, R. Pettman, G. Tanner, C. Mannix, A.A. Culbert, M.J.B. Brown, D.G. Smith, A.D. Reith, The structure of phosphorylated Gsk-3 $\beta$  complexed with a peptide, frattide, that inhibits  $\beta$ -catenin phosphorylation, *Structure* 9 (2001) 1143–1152.
- [30] D. Bossemeyer, R.A. Engh, V. Kinzel, H. Posntingl, R. Huber, Phosphotransferase and substrate binding mechanism of the cAMP-dependent protein kinase catalytic subunit from porcine heart as deduced from the 2.0 Å structure of the complex with adenylyl imidodiphosphate and inhibitor peptide PKI (5-24), *EMBO J.* 12 (1993) 849–859.
- [31] R.N. Armstrong, H. Kondo, J. Granot, E.T. Kaiser, A.S. Mildvan, Magnetic resonance and kinetic studies of the manganese(II) ion and substrate complexes of the catalytic subunit of adenosine 3'-5' monophosphate dependent protein kinase from bovine heart, *Biochemistry* 18 (1979) 1230–1238.
- [32] J. Granot, A.S. Mildvan, E.M. Brown, H. Kondo, H.N. Bramson, E.T. Kaiser, Specificity of bovine heart protein kinase for the delta-stereoisomer of the metal–ATP complex, *FEBS Lett.* 103 (1979) 265–269.
- [33] S. Brenner, Phosphotransferase sequence homology, *Nature* 329 (1987) 21.
- [34] M. Huse, J. Kuriyan, The conformational plasticity of protein kinases, *Cell* 109 (2002) 275–282.
- [35] L. Holm, C. Sander, Mapping the protein universe, *Science* 273 (1996) 560–595.
- [36] P. Cieplak, W.D. Cornell, C.I. Bayly, P.A. Kollman, Application of the multimolecule and multiconformational RESP methodology to biopolymers: charge derivation for DNA, RNA and proteins, *J. Comput. Chem.* 16 (1995) 1357–1377.
- [37] M.J. Frish, et al., 1998. Gaussian Inc., Pittsburgh, PA.
- [38] W.D. Cornell, P. Cieplak, C.I. Bayly, I.R. Gould, K.M. Merz, D.M. Ferguson, D.C. Spellmeyer, T. Fox, J.W. Caldwell, P.A. Kollman, A second generation force field for the simulation of proteins, nucleic acids, and organic molecules, *J. Am. Chem. Soc.* 117 (1995) 5179–5197.
- [39] W.L. Jorgensen, J. Chandrasekhar, J.D. Madura, Comparison of simple potential functions for simulating liquid water, *J. Chem. Phys.* 79 (1983) 926–935.
- [40] AMBER (UCSF): Assisted Model Building with Energy Refinement, version 4.1, Department of Pharmaceutical Chemistry, University of California, San Francisco, 1995. <http://www.amber.ucsf.edu/amber/amber.html>.